In-Orbit Estimation of the Inertia Matrix and Thruster Parameters of UoSAT-12

RE Bordany
Email: R.el-bordany@surrey.ac.uk
Tel: +44 1483 259278 ext. 3411

Willem H. Steyn
Email: H.steyn@eim.surrey.ac.uk
Tel: +44 1483 259278 ext. 3632

M. Crawford
Email: M. Crawford@ee.surrey.ac.uk
Tel: +44 1483 876023

Surrey Space Centre (SSC), University of Surrey, Guildford, GU2 7XH, UK

Abstract

This paper describes a Recursive Least Square (RLS) procedure for use in orbit to estimate the inertia matrix (moments and products of inertia parameters) of a satellite. To facilitate this, one attitude axis is disturbed using a reaction wheel whilst the other two axes are controlled to keep their respective angular rates small. Within a fraction of an orbit three components of the inertia matrix can be accurately determined. This procedure is then repeated for the other two axes to obtain all nine elements of the inertia matrix.

The procedure is designed to prevent the build up of momentum in the reaction wheels whilst keeping the attitude disturbance to the satellite within acceptable limits. It can also overcome potential errors introduced by unmodeled external disturbance torques and attitude sensor noise. The results of simulations are presented to demonstrate the performance of the technique.

The paper also describes an RLS procedure which can be used to estimate the thruster coefficients for thrust levels and alignment of the cold gas thrusters used for attitude control on UoSAT-12. A general on-line method is presented which uses a three axis reaction wheel system to accurately determine the relationship between the commanded and actual torque produced by the thrusters. The calibration algorithm is designed to be robust against external disturbance torques, inertia matrix modelling errors and attitude sensor noise. The results of both simulations and successful in-orbit tests are presented, illustrating the effectiveness of the technique.

I. Introduction

The recent, tendency is to build smaller, lighter and cheaper spacecraft. The present generation of spacecraft require accurate attitude control to provide pointing capabilities. On-line calibration of the attitude control hardware is often necessary to satisfy this high accuracy ADCS requirement. If these systems are not properly calibrated in-orbit, a significant attitude control error can result.

UoSAT-12 is a low-cost 320 kg minisatellite built by Surrey Satellite Technology Ltd. It is a technology demonstrator for high performance attitude control and orbit maintenance for a future constellation of earth observation satellites. The satellite uses a 3-axis reaction wheel configuration and a cold gas thruster system to enable precise and fast control of its attitude. Magnetorquer coils assist the wheels mainly for momentum dumping. Ten cold-gas thrusters can be used in various combinations for both attitude and orbit control and a single N_2O resisto-jet is used exclusively for orbit maintenance.

One of the key features of Surrey's low-cost approach to satellite engineering is the replacement of tight performance requirements and expensive ground calibration campaigns with in-orbit calibration and adaptation. This has been applied extensively to the UoSAT-12 attitude control system, for estimation of the moments of inertia and for calibration of the satellite's thrusters. In this paper, we present two novel RLS

1

methods to identify the spacecraft inertia matrix and the thruster coefficients in-orbit.

Modeling

Dynamic Equations

The dynamic model of an Earth-pointing satellite using 3-axis reaction wheels as internal torque actuators and magnetorquers and thrusters as external torque actuators, is given by:

$$\mathbf{I}\dot{\boldsymbol{\omega}}_B^I = \mathbf{N}_T + \mathbf{N}_M + \mathbf{N}_{GG} + \mathbf{N}_D$$
$$- \boldsymbol{\omega}_B^I \times (\mathbf{I}\boldsymbol{\omega}_B^I + \mathbf{h}) + \mathbf{N}_W \qquad (1)$$

where $\boldsymbol{\omega}_B^I$, $\mathbf{I}$, $\mathbf{h}$, $\mathbf{N}_M$, $\mathbf{N}_T$, $\mathbf{N}_W$, $\mathbf{N}_D$ and $\mathbf{N}_{GG}$ are respectively the inertially referenced body angular velocity vector, moment of inertia of spacecraft, three-axis reaction wheel angular momentum vector, applied torque vector by 3-axis magnetorquers, applied torque vector by 3-axis thrusters, applied torque vector by 3-axis reaction wheels, external disturbance torque vector including the torques due to the aerodynamic and solar forces, and gravity gradient torque vector.

The inertia matrix is defined as,

$$\mathbf{I} = \begin{bmatrix} I_{xx} & -I_{xy} & -I_{xz} \\ -I_{xy} & I_{yy} & -I_{yz} \\ -I_{xz} & -I_{yz} & I_{zz} \end{bmatrix} \qquad (2)$$

Kinematic Equations

The attitude of a satellite can be presented by means of a quaternion [4]. The use of a quaternion in describing the orientation of a rigid body lends itself well to on board calculation since no trigonometric relations or singularities (which arise using Euler angles) exist in the formula, and it can easily be transferred to the orbit-referenced coordinate system. The parameterization of the quaternion vector is

$$q_1 \equiv e_{xo} \sin(\frac{\mathbf{\Phi}}{2}) \qquad q_2 \equiv e_{yo} \sin(\frac{\mathbf{\Phi}}{2})$$
$$q_3 \equiv e_{zo} \sin(\frac{\mathbf{\Phi}}{2}) \qquad q_4 \equiv \cos(\frac{\mathbf{\Phi}}{2}) \qquad (3)$$

where e_{xo}, e_{yo}, e_{zo} are the components of the Euler vector in orbit-referenced coordinates and $\mathbf{\Phi}$ is the rotation angle around the Euler vector. The kinematics can be updated by the following vector set of differential equations:

$$\dot{\mathbf{q}} = \frac{1}{2}\mathbf{\Omega}\mathbf{q} \qquad (4)$$

with,

$$\mathbf{\Omega} = \begin{bmatrix} 0 & W_{oz} & -W_{oy} & W_{ox} \\ -W_{oz} & 0 & W_{ox} & W_{oy} \\ W_{oy} & -W_{ox} & 0 & W_{oz} \\ -W_{ox} & -W_{oy} & -W_{oz} & 0 \end{bmatrix} \qquad (5)$$

where,

$$\boldsymbol{\omega}_B^O = \begin{bmatrix} W_{ox} & W_{oy} & W_{oz} \end{bmatrix}^T$$

is the orbit-referenced angular body rate vector. The transformation matrix to transform any vector from orbital to body-referenced coordinates can be written as:

$$\mathbf{T} = \begin{bmatrix} T_{11} & T_{12} & T_{13} \\ T_{21} & T_{22} & T_{23} \\ T_{31} & T_{32} & T_{33} \end{bmatrix} \qquad (6)$$

Assuming that the satellite is 3-axis stabilized in a circular orbit then,

$$\boldsymbol{\omega}_B^I = \boldsymbol{\omega}_B^O + \mathbf{T}\boldsymbol{\omega}_o \qquad (7)$$

where,

$$\boldsymbol{\omega}_o = \begin{bmatrix} 0 & -W_o & 0 \end{bmatrix}^T$$

is an almost constant orbital angular rate vector.

Error Quaternion

Whenever quaternions are used directly in the attitude control laws, it is convenient to define the error quaternion as the difference between the current quaternion and the commanded quaternion. It can be represented by:

$$\begin{bmatrix} q_{1e} \\ q_{2e} \\ q_{3e} \\ q_{4e} \end{bmatrix} = \begin{bmatrix} q_{4c} & q_{3c} & -q_{2c} & -q_{1c} \\ -q_{3c} & q_{4c} & q_{1c} & -q_{2c} \\ q_{2c} & -q_{1c} & q_{4c} & -q_{3c} \\ q_{1c} & q_{2c} & q_{3c} & q_{4c} \end{bmatrix} \begin{bmatrix} q_1 \\ q_2 \\ q_3 \\ q_4 \end{bmatrix} \qquad (8)$$

where q_{ie} are the components of the error quaternion, q_{ic} the components of the commanded quaternion and q_i the components of the current orbit-referenced quaternion.

II. Controller Design

In this section, we present two feedback control laws that are used to satisfy the requirements of the estimation algorithms during estimation of the inertia matrix and thruster parameters. The satellite is assumed to have a rigid body. The angular velocity vector of the satellite ($\boldsymbol{\omega}_B^O$) is measured or estimated accurately. Its attitude ($\mathbf{q}$) is estimated or measured via the quaternion (4). Consequently, the state vector of the satellite ($\boldsymbol{\omega}_B^O$ and $\mathbf{q}$) is accurately known

2

though subject to sensor noise. The control laws use this state vector to control the satellite's attitude.

The Quaternion feedback Controller

A standard quaternion PD feedback controller consists of linear error-quaternion feedback, with linear and nonlinear body-rate feedback terms to compensate for the gyroscopic coupling torques. The control torque vector is represented as

$$\mathbf{N}_{W/T} = \boldsymbol{\omega}_B^I \times (\mathbf{I}\boldsymbol{\omega}_B^I + \mathbf{h}) - \mathbf{D}\boldsymbol{\omega}_B^O - \mathbf{K}\mathbf{q}_e \qquad (9)$$

where $\mathbf{D}$ and $\mathbf{K}$ are 3×3 constant gain matrices to be properly determined according to Wie[2] and $\mathbf{N}_{W/T}$ the applied torque vector of 3-axis reaction wheels or thrusters.

The Bang-Bang feedback Controller

A Bang-Bang nonlinear controller is implemented using a PD feedback method to control a two level switching control law. The switching function is determined by using a linear feedback equation and a hysteresis band and can be summarized by the following equation:

$$\mathbf{e} = \mathbf{K}_P \mathbf{q}_e + \mathbf{K}_D \boldsymbol{\omega}_B^O$$
$$\mathbf{N}_{W/T} = \begin{cases} -\mathbf{N}_{\max} & \text{for } \mathbf{e} \geq \mathbf{e}_{band} \quad , \text{with } \mathbf{e} \text{ increasing} \\ \mathbf{N}_{\max} & \text{for } \mathbf{e} \leq -\mathbf{e}_{band} \quad , \text{with } \mathbf{e} \text{ decreasing} \end{cases}$$
$$(10)$$

where $\mathbf{K}_P$ and $\mathbf{K}_D$ are controller gains, $\mathbf{e}$ is the control error and $\mathbf{e}_{band}$ is the error hysteresis band. This error band is tuned to adjust the level of the wheel momentum indirectly (and the error quaternion). When reducing the error band the torque output switches at a higher frequency and the wheel momentum build-up is reduced. An increase in the error band has the opposite effect. The controller gains $\mathbf{K}_P$ and $\mathbf{K}_D$ adjust the slope of the switching function, this also controls the stability of the non-linear limit cycle and the magnitude of the error quaternion.

III. Inertia Matrix Identification

In this section, we present a new method for identifying the spacecraft inertia matrix. The way the calibration torque is generated depends on the specific actuators installed on the spacecraft. UoSAT-12, for example, has three reaction wheels. Using accurate wheel speed measurements and knowledge of the wheel moment of inertia, the reaction wheels' torques are accurately known and can be used to estimate the inertia matrix (moments and products of inertia parameters) in-orbit. This is done by disturbing a specific attitude axis using a reaction wheel Bang-Bang controller. The other two axes are controlled using a quaternion feedback controller to control their reaction wheels to keep their respective angular rates small.

This procedure is then repeated for the other two axes to obtain all nine elements of the inertia matrix. Figure 1 summarizes the general in-orbit inertia matrix estimation scheme using reaction wheel actuators. A known disturbance torque $N_{W3}(k)$ is applied to the spacecraft at time k as a result of the Bang-Bang control law, using the third wheel. This torque together with unknown external disturbance torques $\mathbf{N}_D(k)$ and the output from the two-wheel controller $\mathbf{N}_{W12}(k)$ acts on the satellite. The in-orbit moment of inertia calibration procedure (below the dotted line in Fig. 1) uses the known disturbance torque $N_{W3}(k)$, the output from the two wheel controller $\mathbf{N}_{W12}(k)$ and the resulting satellite state to calculate the calibration torque $\mathbf{N}_c(k)$. This calibration torque is used in the measurement equation

$$\mathbf{N}_c(k) = f(\mathbf{I}, \boldsymbol{w}_B^I, \dot{\boldsymbol{w}}_B^I, \mathbf{N}_M, \mathbf{h}, \mathbf{N}_w) \qquad (11)$$

for the RLS algorithm to estimate the inertia matrix $\hat{\mathbf{I}}$ via a suitable high pass filter (see paragraph on high pass filter design).
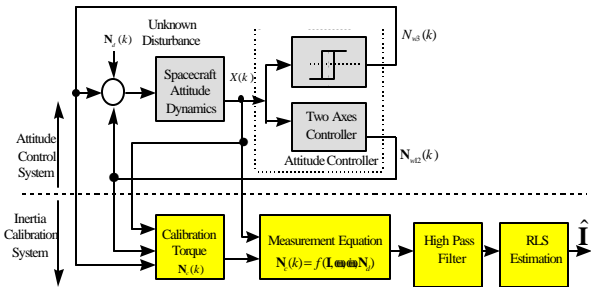

Fig. 1 On-orbit inertia matrix estimation block diagram

Reduced Equations of motion

This novel moment of inertia (MOI) estimation algorithm depends on the idea that when disturbing one axis using the corresponding wheel, the principal moment of inertia can easily be estimated. By keeping the angular rate disturbances in the other two axes close to zero using the quaternion feedback controllers and combining the dynamic equations of these two axes we can estimate the products of inertia.

A problem for nadir pointing satellites is that the inertial angular rate in the Y-axis (pitch) is non-zero and equal to the orbital rate. It is therefore recommended first to disturb the Y-axis and control the X and Z-axes, keeping the angular rates in these axes close to zero. This will reduce the cross coupling in the dynamic equations between the Y-axis and the other two axes, so that the products of inertia terms when estimating I_{yy}, I_{xy} and I_{yz} are negligible. The second step will be to disturb the X or Z-axis and to control the remaining two axes.

The dynamic model of an Earth-pointing satellite using 3-axis reaction wheels as internal torque actuators, and

3

magnetorquers as external torque actuators, is given in (1). It is clear from these dynamic equations that it is better to estimate the principle moment of inertia terms by disturbing the satellite using a small level of reaction wheel torque and momentum. This decreases the effect of the products of inertia in the dynamic equations, but ensures sufficient torque and momentum to counteract the influence of unknown external disturbance torques [5]. Conversely, when estimating the products of inertia it is better to disturb the satellite using full reaction wheel torque and momentum in order to increase the influence of the products of inertia in the dynamic equations.

The presence of external disturbance torques tends to cause wheel momentum drift. Therefore, management of reaction wheel momentum is required in order to counteract the influence of persistent external disturbance torques. On UoSAT-12 an external torque using magnetorquers is applied for wheel momentum management. This also ensures that the satellite angular rate values in the two controlled axes are kept close to zero. Furthermore, small angular rates in the controlled axes will decrease the effect of cross-coupling and result in improved estimates of the products of inertia.

Case Study: Disturb Y-axis and Control X and Z axes

Neglecting small terms, the reduced dynamic equations of motion (1) describe the effect of disturbing the Y-axis using the reaction wheel Bang-Bang controller (10) and controlling the X and Z axes using quaternion feedback reaction wheel controllers (9), (with momentum dumping) and can be written as thus:

$$I_{xx}\dot{w}_x = N_{mx} + I_{xy}\dot{w}_y + w_y^2 I_{yz} + w_z h_y - w_y h_z - \dot{h}_x \quad (12\text{-a})$$

$$I_{yy}\dot{w}_y = N_{my} - w_z h_x + w_x h_z - \dot{h}_y \quad (12\text{-b})$$

$$I_{zz}\dot{w}_z = N_{mz} + I_{yz}\dot{w}_y - w_y^2 I_{xy} - w_x h_y + w_y h_x - \dot{h}_z \quad (12\text{-c})$$

Two separate RLS estimations are needed for each axis: One to estimate the principle moment of inertia I_{yy}, and the other to estimate the products of inertia I_{xy} and I_{yz}.

For the first of these rewrite (12-b) in the form

$$N_{cy}(k) = I_{yy}\dot{w}_y \quad (13)$$

where, $N_{cy}(k)$ is the calibration torque required to estimate I_{yy} and is given by:

$$N_{cy}(k) = N_{my} - w_z h_x + w_x h_z - \dot{h}_y \quad (14)$$

Equation (13) acts as the measurement equation for the RLS estimation to estimate I_{yy}. The error to be minimized can be written as:

$$e_y(k) = N_{cy}(k) - \hat{I}_{yy}\dot{w}_y(k) \quad (15)$$

Where $\hat{I}_{yy}$ is the estimated inertia parameter.

For the second RLS to estimate I_{xy} and I_{yz} adding (12-a) and (12-c) and rearranging gives:

$$N_{cyp}(k) = \hat{I}_{xy}(\dot{w}_y - w_y^2) + \hat{I}_{yz}(\dot{w}_y + w_y^2) \quad (16)$$

where, $N_{cyp}(k)$ is the calibration torque given by:

$$N_{cyp}(k) = \hat{I}_{xx}\dot{w}_x + \hat{I}_{zz}\dot{w}_z - N_{mx} - N_{mz} - \\ - h_y(w_z - w_x) - w_y(h_x - h_z) + \dot{h}_x + \dot{h}_z \quad (17)$$

and $\hat{I}_{xx}, \hat{I}_{zz}$ can be obtained from an initial estimate.

Equation (16) also acts as the measurement equation for the RLS estimation to estimate I_{xy} and I_{yz}. The error to be minimized can be written as:

$$e_{yp}(k) = N_{cyp}(k) - \hat{I}_{xy}(\dot{w}_y - w_y^2) - \hat{I}_{yz}(\dot{w}_y + w_y^2) \quad (18)$$

in practice, both error equations (15) and (18) are high pass filtered to remove the effects of low frequency disturbance torques. This procedure is then repeated for the other two axes to obtain all nine elements of the inertia matrix. The results of the estimated products of inertia from any two-axes can then be compared to ensure that the values of the products of inertia are estimated correctly.

RLS Implementation

The inertia matrix identification can now be formulated as follows: Given the measurement equations (13) and (16) estimate the mean values of the inertia matrix $\hat{\mathbf{I}}$. A RLS calibration algorithm based on real time parameter estimation is proposed for improved convergence and accuracy. The algorithm is a recursive implementation of the least squares minimization technique and is appropriate because of the almost time invariant nature of the inertia parameters (2). The error to be minimized can be written as a standard least square parameter estimation problem:

$$e_i(k) = y_i(k) - \varphi^T_i \theta_i(k) \quad (19)$$

The least squares cost function to be minimized is taken as:

$$J = \frac{1}{2}\sum \mathbf{l}^{t-k} e_i^2(k) \quad (20)$$

The forgetting factor $\mathbf{l}$ is a constant ($\mathbf{l} \leq 1$) which defines the smoothing of the estimates by introducing a time varying weighting of data. The full RLS algorithm will be given as,
- Compute the regression vector $\varphi_i(k)$ and the residual $e_i(k)$ from (19)
- Compute the update gain vector

$$\mathbf{K}_i(k) = \mathbf{P}_i(k-1)\boldsymbol{\varphi}_i(k)[\boldsymbol{I} + \boldsymbol{\varphi}_i^T(k)\mathbf{P}_i(k-1)\boldsymbol{\varphi}_i(k)]^{-1}$$

(21)

Where, $\mathbf{P}_i$ is defined as the covariance matrix of the parameter vector $\boldsymbol{\theta}_i(k)$

- Update the parameter vector

$$\boldsymbol{\theta}_i(k) = \boldsymbol{\theta}_i(k-1) + \mathbf{K}_i(k)e_i(k)$$

(22)

- Update the covariance matrix

$$\mathbf{P}_i(k) = [\mathbf{I} - \mathbf{K}_i(k)\boldsymbol{\varphi}_i^T(k)]\mathbf{P}_i(k-1)/\boldsymbol{I}$$

(23)

Addition Error Processing

The above general RLS procedure is further modified by processing the error to remove low frequency components and outlying values. To improve the robustness of the RLS algorithm, the error can be modified by a non-linear saturation function (see Steyn [3]) as follows:

$$f\{e_i(k)\} = \frac{e_i(k)}{1 + b|e_i(k)|}$$

(24)

The constant b is defined such that the function is still linear for normal values of $e_i(k)$, while decreasing the influence of large outliers.

High pass filter design

Low frequency (e.g. Aerodynamic) disturbance torques influence the satellite states (angular rate, quaternion) which are used by the attitude controller to control the satellite with corresponding reaction wheel torque and momentum. All these disturbance terms form part of the RLS error but can be filtered out using a second order Butterworth high pass filter during MOI calibration. This is the best location for the high pass filter because the error contains all the parameters affected by the low frequency disturbance torques (reaction wheel torque, wheel momentum, angular rate and angular acceleration).

IV. Thruster Coefficients Identification

Following an idea of Wiktor [1] , a novel RLS algorithm can be used to calibrate the cold gas thrusters in-orbit during normal mission conditions, when the satellite is stabilised. This method requires knowledge of a calibration or known disturbance torque (generated using reaction wheel actuators on UoSAT-12) whilst the attitude is controlled using the gas thrusters.

The n thrusters are controlled by n commands in vector $\mathbf{T}_c$ from the attitude controller. The resultant torque $\mathbf{N}_T$ exerted on the spacecraft from this set of thruster commands is

$$\mathbf{N}_T = \mathbf{A}\mathbf{T}_c$$

(25)

where $\mathbf{N}_T$ is a 3×1 vector, and $\mathbf{A}$ the $3 \times n$ thruster configuration matrix which contains the information about the output direction and magnitude of each thruster. The goal of the thruster calibration is to identify these $3 \times n$ coefficients in spite of sensor noise and external disturbance torques.
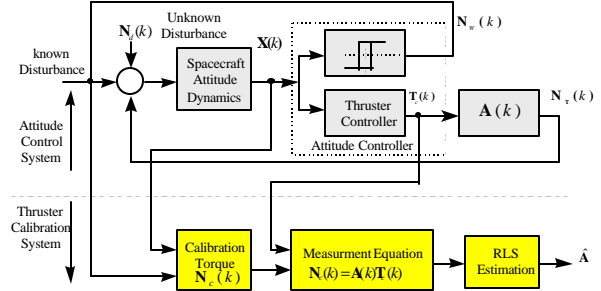
Calibration Techniques

Fig. 2 On-orbit thruster calibration block diagram

Figure 2 summarises the general in-orbit thruster calibration scheme. A known disturbance torque $\mathbf{N}_W(k)$ is applied to the spacecraft using reaction wheels controlled by a Bang-Bang control law (10), whilst the attitude controller (9) sends commands $\mathbf{T}_c(k)$ to the thrusters (generating torques $\mathbf{N}_T(k)$) to compensate for both this known and also any unknown external disturbance torques $\mathbf{N}_D(k)$.

The in-orbit thruster calibration procedure (below the dotted line in Fig. 2) uses the known disturbance torque $\mathbf{N}_W(k)$ and the resulting measured satellite state to calculate the calibration torque $\mathbf{N}_c(k)$ acting on the satellite. This calibration torque is equal to the sum of the known and the unknown disturbance torques and can be obtained by rearranging equation (1) thus

$$\mathbf{N}_c = \mathbf{I}\dot{\boldsymbol{\omega}}_B^I + \boldsymbol{\omega}_B^I \times (\mathbf{I}\boldsymbol{\omega}_B^I + \mathbf{h}) - \mathbf{N}_W$$

(26)

so that it also includes the effects of measurement noise in estimating the state. If the satellite attitude is maintained, this torque is being exactly cancelled by the thruster torque given by (25), so to estimate $\mathbf{A}$, rewrite (25) as a state estimation problem with the measurement equation

$$\mathbf{N}_c = \hat{\mathbf{A}}\mathbf{T}_c + \mathbf{n}$$

(27)

where $\mathbf{n}$ is the effect of measurement noise plus the external disturbance torques and $\hat{\mathbf{A}}$ is the estimated value of the true thruster coefficient matrix $\mathbf{A}$.

The objective of the thruster calibration procedure is to estimate the mean value $\hat{\mathbf{A}}$ of the true thruster coefficient matrix $\mathbf{A}$ which should not change with time, so they can be modeled by the state equation

5

$$a_{ij}(k+1) = a_{ij}(k) \tag{28}$$

where a_{ij} is an element of the estimated thruster coefficient matrix $\hat{\mathbf{A}}$. The thruster calibration problem can now be formulated using (27) and (28) as an RLS calibration algorithm based on real time parameter estimation.

V. Simulation Results

In this section, we present simulation results to identify both the thruster parameters and the spacecraft inertia parameters. Simulations were performed using MATLAB and SIMULINK. The RLS algorithms were implemented using a full simulation of the satellite dynamics, sensors and environmental models. The UoSAT-12 satellite in a LEO was used as an example during these simulations to test the new algorithms. The parameters used during the simulation are summarized in Table 1. The estimation algorithms were run both with and without aerodynamic disturbance torque. During the simulation a set of three thrusters pairs were used to test the thruster algorithm to identify the 3×3 calibration matrix $\hat{\mathbf{A}}$.

Figure 3 illustrates the performance of the RLS MOI estimation algorithm without aerodynamic disturbance when disturbing the Y-axis and controlling the X and Z axes. It is clear from these figures that the convergence of the RLS estimated parameters was achieved in approximately 1000 seconds in the case of the moment of inertia I_{yy} and approximately 3000 seconds in the case of the products of inertia I_{xy} and I_{yz}. The parameter variation after convergence was very small around the true value. Figure 5 illustrates the performance with a non-zero mean aerodynamic disturbance torque (see Figure 14). It is clear from this figure that the convergence rates are somewhat slower than the case without aerodynamic disturbance torques, Figure 3, (I is the same) but that parameter convergence will still occur. This slower convergence is due to the drift in the reaction wheel momentums, (compare Figures 4 and 6) when compensating for the external disturbance torque and consequent build-up in the angular rates in X and Y axes. This also increases the effect of cross-coupling, resulting in a slower convergence of the estimates of the products of inertia.

Figures 7 and 8 illustrate the performance of the RLS algorithm to estimate the thruster coefficients with and without aerodynamic disturbance torque. It is clear from these figures that the results are almost identical and the thruster parameters converge to the true values in less than half an orbit.

VI. In-Orbit Results

In this section, we present the identification of thruster coefficients using real data generated on board UoSAT-12.

The thrust arm of the roll, pitch and yaw thrusters (8 cold gas) to the CoG of UoSAT-12 is approximately 0.44 m each, giving a torque of 35 milli-Nm for attitude control. The Z-axis (yaw) control thrusters will, however, always be fired simultaneously in an opposing pair to give a pure rotation without any translation force, so the Z-axis thruster torque will be 70 milli-Nm per dual pulse (see figure 13 for the location of yaw-thrusters). A pair of thrusters are implemented to generate attitude control rotation of the satellite around the yaw-axis, the other two axes being controlled using reaction wheel actuators to identify the 3×2 coefficients of the Z-thrusters (29).

$$\mathbf{N}_T = \begin{bmatrix} a_{xzp} & a_{xzn} \\ a_{yzp} & a_{yzn} \\ a_{zzp} & a_{zzzn} \end{bmatrix} \begin{bmatrix} T_{zp} \\ T_{zn} \end{bmatrix} \tag{29}$$

where, T_{zp} and T_{zn} refers to positive and negative firing torque respectively (nominal magnitude of 70 milli-Nm).

Figures 11 and 12 illustrate the satellite angular rate and wheel momentum respectively during the experiment). We observe from Figure 9 that the mean values of the positive thruster coefficients converge approximately to 0.01,-0.087,1 while the mean values of the negative thruster coefficients converge approximately to 0.03,0.13,0.72 for the X, Y and Z axes respectively. Finally the estimated thruster coefficients were used to identify the principle moment of inertia of the Z-axis. We observe from Figure 10 that the mean value of the principle moment of inertia I_{zz} converges to its measured value with small variation around the measured value.

VII. Conclusions

Two novel RLS algorithms have been presented to identify satellite inertia matrix and thruster parameters in-orbit. Both algorithms assume no knowledge of the thruster parameters and only an initial guess of the inertia matrix. Numerical simulations illustrate the successful identification of the thruster parameters and inertia matrix in spite of non-zero mean disturbance torques and sensor noise. In orbit tests have been shown to confirm the operation of the thruster identification technique. The RLS estimation algorithms could be applied in real-time on board a LEO nadir pointing satellite in order to improve the attitude control performance.

References

1. Wiktor, P.J. "On-Orbit Thruster Calibration", Journal of Guidance, Control and Dynamics, Vol. 19, No.4, July.-August. 1996, pp. 934-940.

2. Wie, B., Weiss, H. and Arapostathis, A. "Quaternion Feedback Regulators for Spacecraft Eigenaxis Rotations", Journal of Guidance, Control and Dynamics, Vol. 12, No.3, May.-June. 1989, pp. 375-380.

3. Steyn, W.H., "A Multi-mode Attitude Determination and Control System for Small Satellites", PhD thesis, University of Stellenbosch, December 1995.

4. Wertz, J.R., Spacecraft Attitude Determination and Control, D. Reidel Publishing Company, Dordrecht, Holland, 1989.

5. Bshrivastava, S.K. and Modi, V.J. "Satellite Attitude Dynamics and Control in the Presence of Environmental Torques—A Brief Survey", Journal of Guidance, Control and Dynamics, Vol. 6, No.6, Nov.-Dec. 1983, pp. 461-471.

Refaat El-Bordany received the B.S. degree in electronic engineering from the Military Technical University in 1989, the M.S. degree in electrical engineering from Military Technical University 1996, Cairo. He is currently studying for Ph.D. degree in spacecraft attitude control system at the Surrey Space Centre of University of Surrey in UK.

Willem H. Steyn is the team leader for AODCS at SSTL. Previously he was a Senior Lecturer in Electronic Engineering at the University of Stellenbosch in South Africa. His primary research fields are satellite control, actuators and sensors. He received his Honors, Masters and Ph.D degrees in Electronic Engineering from the University of Stellenbosch and a M.Sc in Satellite Engineering from the University if Surrey. The title of his Ph.D is "A Multi-mode Attitude Determination and Control System for Small Satellites".

Mike J. Crawford has lectured on topics in Control Engineering and in Electronics Design on courses in the Department of Electronic Engineering at the University of Surrey for twenty years. He is now on the academic staff of the Surrey Space Centre with interests in research on a variety of topics in satellite attitude control systems and in the design of electronics for satellite sensor and power systems.
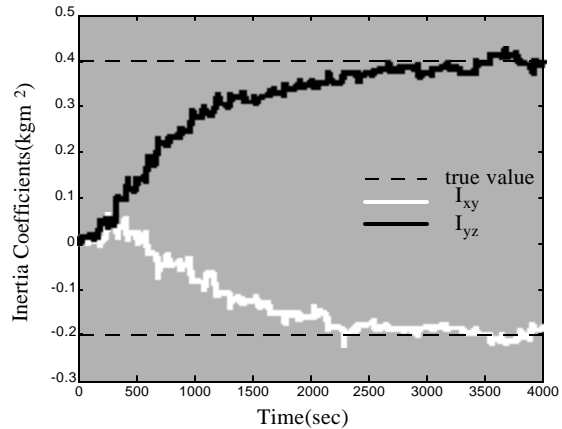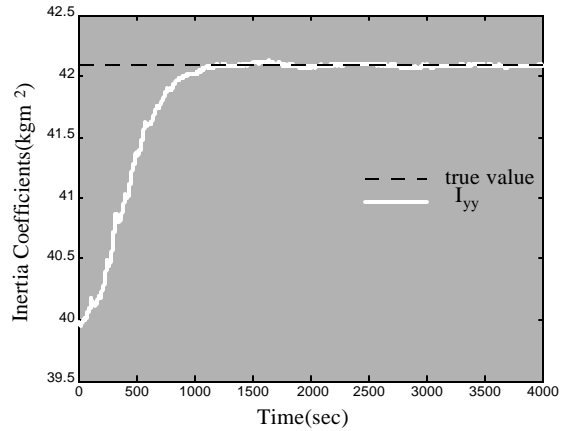
Figure 3 Estimated inertia without aerodynamic disturbance

7
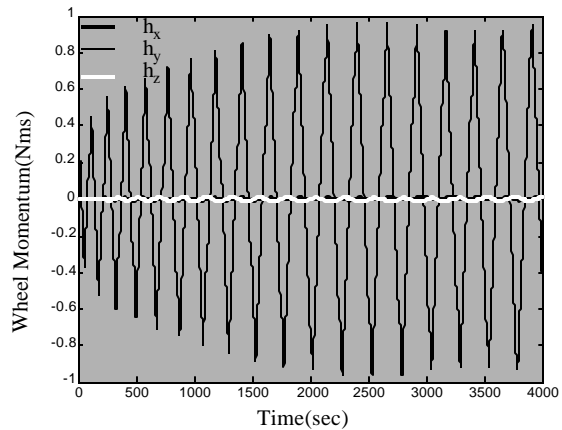
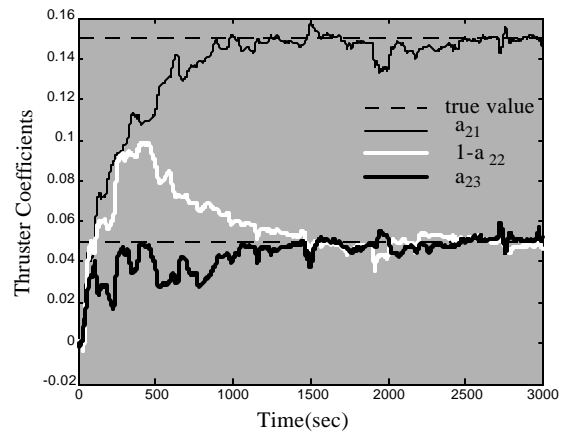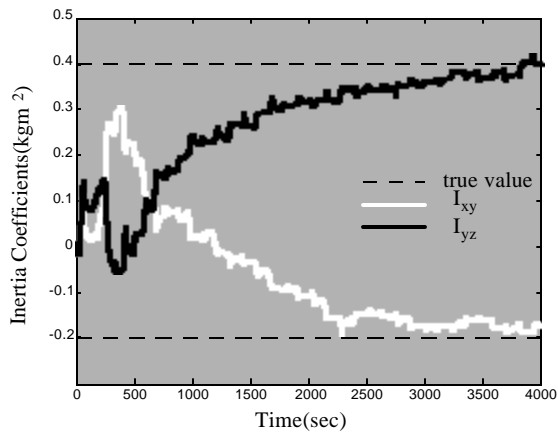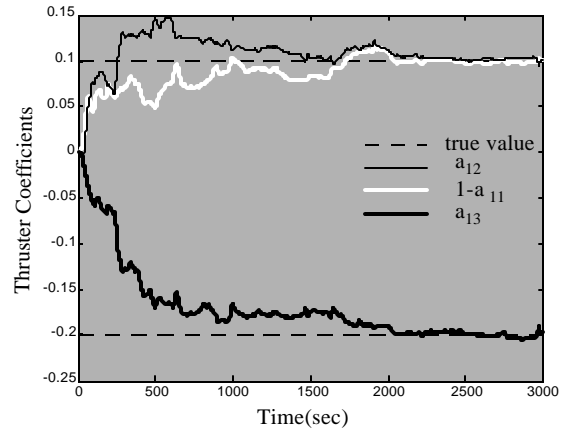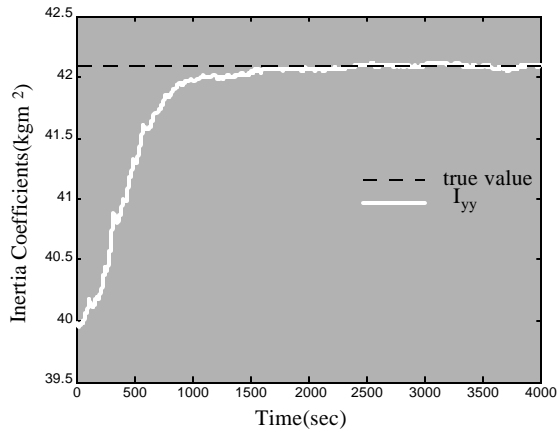Figure 4 Reaction wheel angular momentum without aerodynamic disturbance
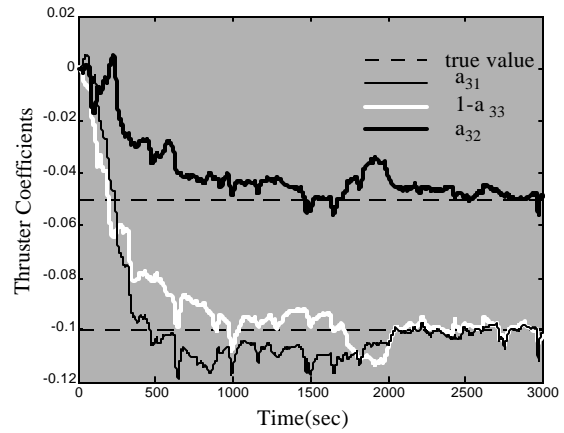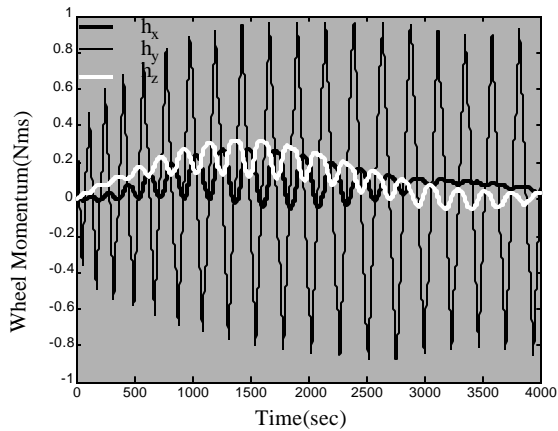

Figure 5 Estimated inertia with aerodynamic disturbance

Figure 6 Reaction wheel angular momentum with aerodynamic disturbance

Figure 7 Estimated thruster coefficients without aerodynamic disturbance
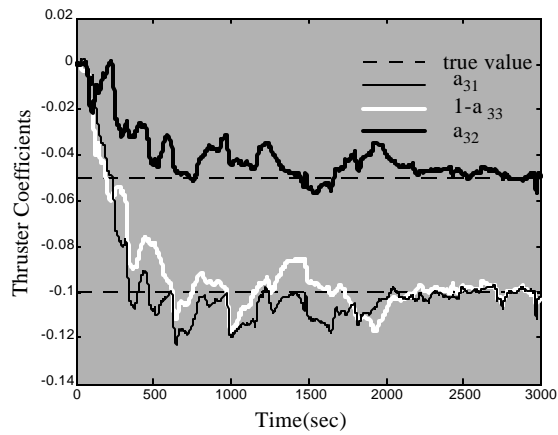
8

Figure 9 Estimated Thruster Coefficients
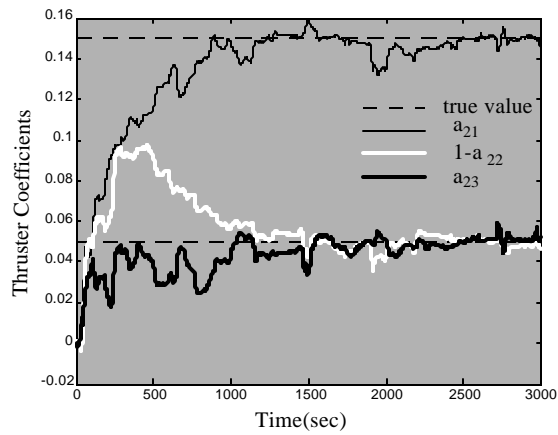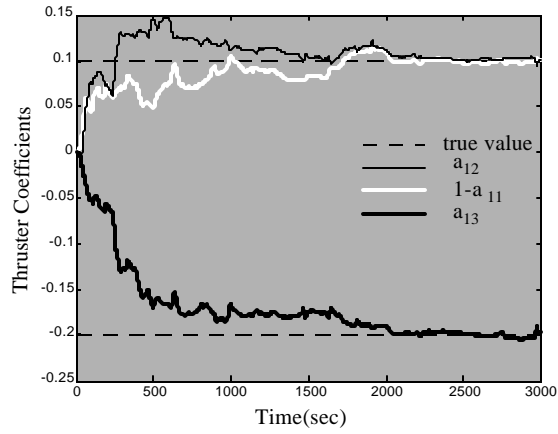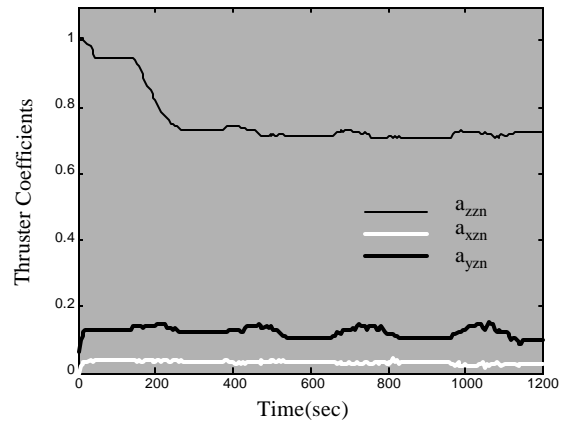for the UoSAT-12

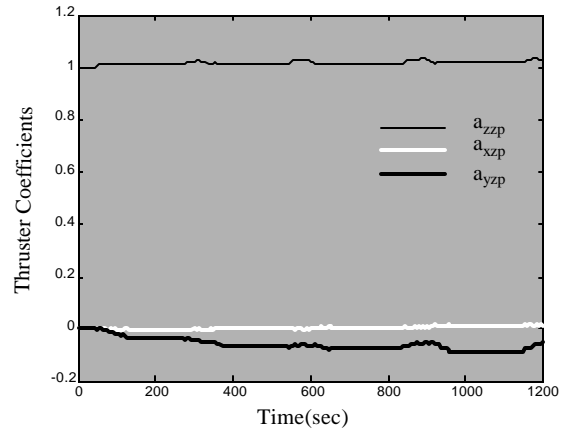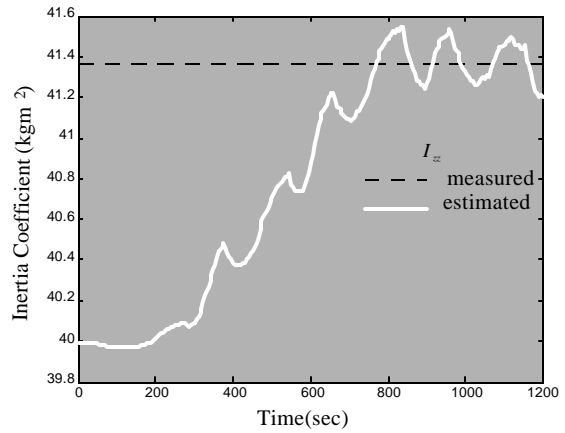Figure 8 Estimated Thruster Coefficients with
aerodynamic disturbance

Figure 10 Estimated moment of Inertia
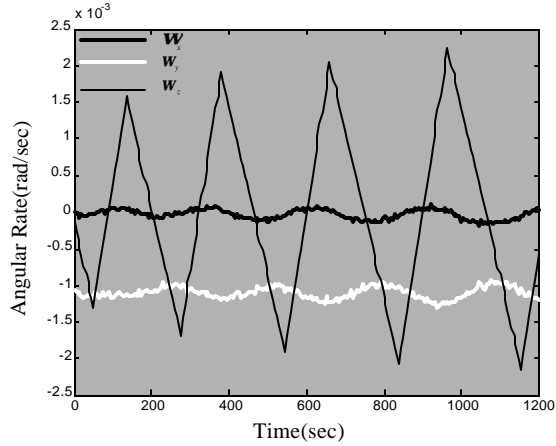for the UoSAT-12
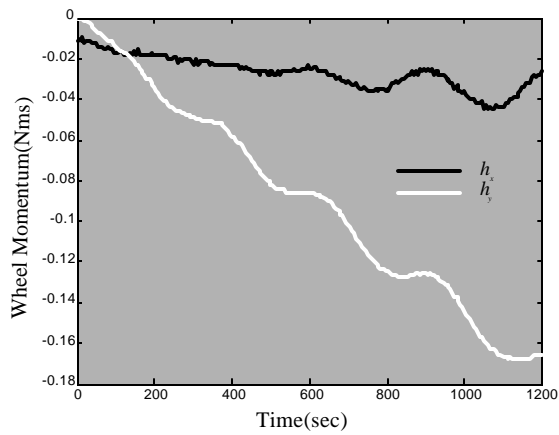
9

Figure 11 Angular Rate for the UoSAT-12
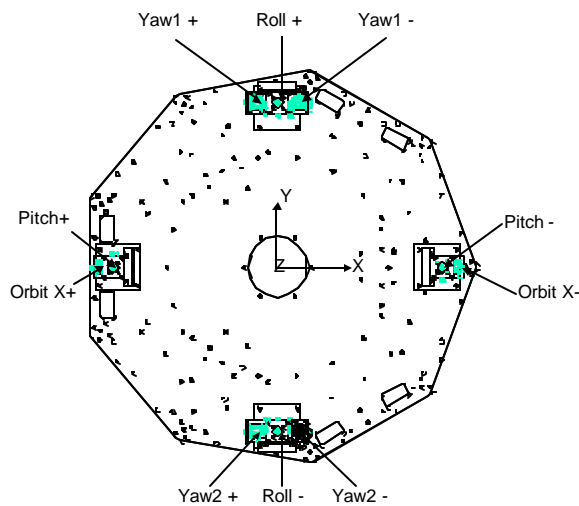

Figure 12 Reaction wheel Momentum for the
UoSAT-12

Figure 13 Top view of cold gas thrusters
for UoSAT-12

Table 1 UoSAT-12 simulation parameters

| Moment of Inertia Tensor	$\mathbf{I} = \begin{bmatrix} 40.45 & -0.2 & -0.5 \\ -0.2 & 42.09 & 0.4 \\ -0.5 & 0.4 & 41.36 \end{bmatrix} kg.m^2$
Orbital parameters	Orbital rate $= 2\pi / 6000$ rad/sec Inclination i $= 65^0$ Orbital Period $= 100$ min
Sample time	1 sec
Cold gas thruster	Torque output 0.035 Nm Minimum firing-time $= 20$ milli-seconds
Reaction wheel	Maximum torque $=0.015$ Nm Maximum Momentum $= 4$ Nms Moment of inertia $= 0.0077$ kgm^2 Maximum speed $= 5000$ rpm
Thruster Coefficients	$\mathbf{A} = \begin{bmatrix} 0.9 & 0.1 & -0.2 \\ 0.15 & 0.95 & 0.05 \\ -0.1 & -0.05 & 1.1 \end{bmatrix}$
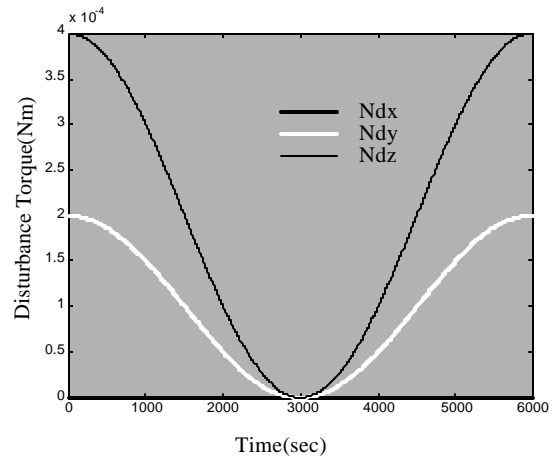
Figure 14 Aerodynamic disturbance torque

10